Postharvest Biology and Technology 51 (2009) 391–398

Contents lists available at ScienceDirect

Postharvest Biology and Technology

journal homepage: www.elsevier.com/locate/postharvbio

Comparative studies on nanostructures of three kinds of pectins in two peach cultivars using atomic force microscopy

Hongshun Yang[a,*], Fusheng Chen[a], Hongjie An[a], Shaojuan Lai[b]

[a] College of Food Science and Technology, Henan University of Technology, 140 South Songshan Road, Zhengzhou, Henan 450052, China
[b] Department of Biochemistry, Molecular Biology and Biophysics, University of Minnesota-Twin Cities, Minneapolis, MN 55455, USA

ARTICLE INFO

Article history:
Received 1 May 2008
Accepted 22 August 2008

Keywords:
Nanotechnology
Atomic force microscopy (AFM)
Pectin
Firmness
Peach
Nanostructure

ABSTRACT

Firmness is an important postharvest quality property of fruit. To investigate the reasons for firmness differences between soft and crisp fruit cultivars, two peach (*Prunus persica* L. Batsch) cultivars (soft and crisp) were selected to compare the nanostructures of pectins. Water-soluble pectin (WSP), chelate-soluble pectin (CSP) and sodium carbonate-soluble pectin (SSP) were extracted and nanostructures were conducted and analyzed using atomic force microscopy (AFM). The results show that SSP chain lengths were different between the two cultivars with average SSP lengths of 249 nm and 57 nm for fruit of the crisp and soft cultivars, respectively, while the WSP and CSP chain lengths were not much different. There were no statistical differences for chain heights and widths in the three kinds of pectins between fruit of the two cultivars. All the chain heights were about 1–5 nm. The results indicate that neutral sugar-rich pectins from the primary cell wall of peach flesh might be the cause of the main differences in pectin nanostructures between the two cultivars. The neutral sugar-rich pectins in primary cell walls of peach might also be the reason for firmness differences.

1. Introduction

Maintaining a reasonable level of firmness is very important for achieving high market value for fruit (Zhou and Li, 2007). Changes in cell wall structures and composition contribute markedly to fruit softening (Ali et al., 2004; Yang et al., 2008), with solubilisation of pectin, one of the important cell wall polysaccharides in the middle lamella, considered the primary reason for fruit softening (Ketsa et al., 1999). Furthermore, pectin plays many other important roles in fruit cells including affecting cell wall porosity, adjusting cell wall pH and charge, regulating inter-cell adhesion, and in pathogen defense signalling (Fishman et al., 2004), as well as serving as structural elements and contributing significantly to the texture of processed and fresh fruit (Fishman et al., 1992). Chemical analysis shows that pectin contents in fruit change with softening, but the degree of the change varies among fruit (Ali et al., 2004; Deng et al., 2005). Firmness of fruit is also related to the structural integrity of constituent pectin (Yang et al., 2006c).

Pectin is a heterogeneous polysaccharide. Varying structures or complex repeat units make them hard to be characterized by most current physical and chemical methods, and generally only whole-sample based information can be obtained (Round et al., 1997; Yang et al., 2007). Microscopy has an advantage over other physical characterization techniques in that it can visualize heterogeneity of the sample directly (Ikeda et al., 2001; He et al., 2004). Atomic force microscopy (AFM), as a nanotechnology approach, is a powerful and useful tool for studying food and biological materials (Morris et al., 2001). It allows high magnification with high resolution, three-dimensional imaging and measurement of samples with minimal preparation in different media, permitting direct observation of specimens under near-native conditions (Yang et al., 2005b, 2007). Previous research using AFM showed qualitative and some quantitative aspects of pectin polymers of fruit during storage (Yang et al., 2005a, 2006b,c). However, aggregation of pectin molecules or entanglement of pectin linear molecules resulted in potentially observable molecular features being obscured. Manipulation could extend the pectin chains and provide an opportunity to determine the length of pectin molecules directly. The combing technique we developed can separate intramolecular aggregates rather than intermolecular ones. For instance, if calcium facilitated association is intermolecular, the association should be separated by this technique. It can be applied to stretch the pectin chains as well as the pectin molecules from the chelator solutions or sodium carbonate solutions (Yang et al., 2006a). Based on the developed pectin molecular manipulation technologies, the relationship between nanostructure and firmness of fruit can be investigated. Preliminary results from Chinese cherry showed that firmness was

* Corresponding author. Tel.: +86 371 67789991; fax: +86 371 67756856.
E-mail addresses: yhsfood@haut.edu.cn, hongshunyang@hotmail.com (H. Yang).

0925-5214/$ – see front matter © 2008 Elsevier B.V. All rights reserved.
doi:10.1016/j.postharvbio.2008.08.009

closely related to the nanostructures of sodium carbonate-soluble pectin (SSP) at different ripening stages (Zhang et al., 2008).

The purpose of this research was to investigate the nanostructural differences of different pectin fractions (water-soluble pectin (WSP), chelate-soluble pectin (CSP) and SSP) and between different peach cultivars (crisp and soft). The qualitative and quantitative nanostructural results of the peach pectins were compared and analyzed. The results will help to clarify the relationship between pectins and firmness of fruit, and will be beneficial in directing the storage and handling of peaches for maintaining good texture.

2. Materials and methods

2.1. Fruit material

Two cultivars (crisp 'Jinxiu' and soft 'Milu') of peach (*Prunus persica* L. Batsch) were used for the experiments. The peaches were selected at a commercial maturity stage as determined by experienced farmers. The peaches were bought from the market and were transferred to the laboratory. Peaches of uniform size, free of disease and without other defects were selected. The peaches were then cooled for 12 h at 4 °C. The two cultivars were designated as soft and crisp peaches according to their textural differences as described below. The peaches were then stored at 20 °C for 6 d for ripening. Then the peaches were subjected to the following experimental protocol.

2.2. Cell wall preparation and pectin extraction

The WSP, CSP and SSP were extracted according to a published method (Zhou et al., 2000) with slight modifications (Yang et al., 2005a, 2006b,c). Peaches from the two cultivars were peeled and about 5.5 g flesh from each cultivar were used for extracting cell wall materials. The flesh was boiled in ethanol for 20 min, and after filtration the pellet was transferred to 20 mL ultra-purified water (Milli-Q Biocel Pure Water Equipment, Millipore Co. Ltd., France). After 2 h extraction with agitation on a shaker, the supernatant was collected as WSP and the pellet was washed with acetone, then with 1:1 chloroform:methanol (v/v). The pellet was then resuspended in 20 mL 50 mM *trans*-1,2-diaminocyclohexane-*N*,*N*,*N*′,*N*′-tetraacetic acid (CDTA) and shaken for 3 h. After that it was centrifuged (Beijing Medical Equipments Co. Ltd.) at 15,000 × *g* for 10 min, and the supernatant was collected and the pellet was extracted twice more with 10 mM CDTA. The three supernatants were collected as the CSP fraction. The pellet was then resuspended in 20 mL 50 mM Na_2CO_3 and 20 mM $NaBH_4$ with agitation at 4 °C for 18 h, then transferred to room temperature for 2 h, centrifuged at 15,000 × *g* for 10 min, and extracted twice more with 20 mL of the above Na_2CO_3 solution. The three supernatants were adjusted to pH 7.0 with acetic acid and the SSP fraction was thus obtained.

2.3. AFM imaging

AFM was conducted in a glove box at 30–40% relative humidity and about 25 °C. The relative humidity inside the glove box was adjusted by silica gel and maintained at a stable level for at least 5 h prior to AFM observation (Yang et al., 2006c). Tapping mode was performed using a Multimode AFM (NanoScope IIIa, Veeco/Digital Instruments, Santa Barbara, CA, USA) equipped with a J or E scanner. The scanner could be adjusted to select and capture smaller images within the region accessible for scanning. The NSC 11/no Al tip (MikroMasch, Wilsonville, Oregon, USA) with a resonance frequency of 330 kHz was used. The force constant (determined by the dimensions and material) of the cantilever B of the tip was 48 N/m, which was provided by the manufacturer of the AFM tip. A scan speed of ~2 Hz was applied for imaging (Yang et al., 2005a, 2006b,c). Before imaging each sample, the AFM tip was checked for contamination by laser scanning, that is, the integrity of the AFM tip was checked. The integrity was verified by imaging a reference standard with a known roughness and surface morphology that was provided by the manufacturer. If the tip was contaminated, the AFM images of the reference standard would deviate from the images provided by the manufacturer and thus a new tip for imaging would be used (Reed et al., 1998).

The pectin solutions were allowed to recover at room temperature and were disrupted for several minutes using a XW-80A Vortex mixer (Shanghai Jinke Co., Ltd., Shanghai, China). Then, a small volume (about 20 μL) of the solution was pipetted rapidly (for about 5 s) onto the freshly cleaved mica surface. Modified molecular combing was exerted, with a glass cover slip to comb the solutions and extra pressure with a finger on the glass cover slip was applied while combing. The manipulation should be accomplished in several seconds in case pectin molecules conglomerate (Yang et al., 2006a). The mica surface was then dried by forced air using an ear syringe. The concentrations of the pectin solutions could be modified according to the imaging for obtaining images of individual polymers (Yang et al., 2006c).

Height images in the tapping mode were applied which maximally recorded the true topography of soft samples (Decho, 1999). Advantages of the tapping mode were the low force and minimal damage for imaging soft samples in air. Furthermore, lateral forces are greatly eliminated so that deformation of the sample was minimal and high lateral resolution was obtained (Fishman et al., 2004).

2.4. AFM image analysis

AFM images were analyzed off-line using the NanoScope software (version 5.30b4) provided by the manufacturer. The function of flattening by the software reduced the noise of the samples and obtained high quality images, and it hardly changed the quantitative results of the dimensions of the samples. The bright and dark areas in the AFM images corresponded to high and low parts in the observed samples. It should be noted that different scales were used in the vertical (about several microns) and horizontal axes (about several nanometers), and the height mode images were used for the analysis (Yang et al., 2006c). Both qualitative and quantitative information could be obtained. At true branch points, the height of the molecule will remain unchanged, while two molecules crossover each other, then the measured height will double (Round et al., 2001). The dimensions of the pectin (length, width and height) were determined using section analysis of the AFM software. The width and height of a single strand were determined by measuring the horizontal distance and vertical distance, respectively (Gunning et al., 2003; Yang et al., 2006c). The lengths of individual pectin chains were obtained by tracing along the chain length (Ikeda et al., 2004b).

2.5. Statistical analysis

Sample preparation and measurements were determined at least in triplicate. Statistical analyses using analysis of variance (ANOVA) ($P < 0.05$) and Duncan's multiple range test for differences in the quantitative dimensions of pectin chains were performed using SAS software (Version 9.1.3, SAS, Cary, NC, USA). Comparisons that yielded $P < 0.05$ were considered significant.

3. Results

3.1. Qualitative results

Fig. 1 shows the tapping mode AFM height images of WSP chains of fruit of the two peach cultivars. Figs. 2 and 3 show the

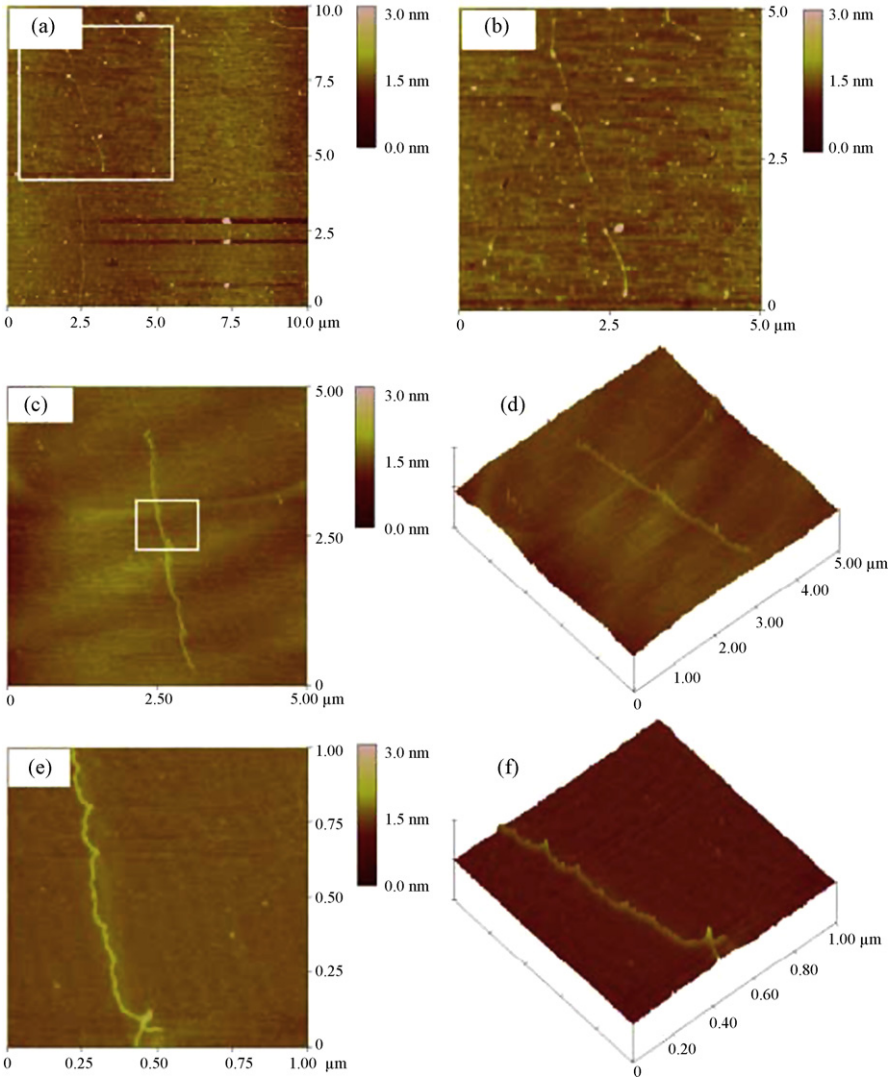

Fig. 1. AFM images of water-soluble pectin (WSP) from soft and crisp peach cultivars. (a) WSP from crisp peaches; (b) an enlarged image of (a); (c) WSP from soft peaches; (d) corresponding 3D image of (c); (e) an enlarged image of (c); (f) corresponding 3D image of (e).

corresponding CSP and SSP data, respectively. The figures reveal that the length and width of the chains were different, which indicates that the pectin structure was heterogenic. It was not clear whether the shorter length chains (Fig. 2b, for instance) were broken from the main chain or whether they existed as a separate chain in the flesh (Arnaudov et al., 2003). We should mention that since the solutions for the AFM imaging were extracted without dialysis, the chelator and the sodium carbonate were left in the solutions and appeared on the AFM images (Figs. 2a and d and 3d), and the images represented genuine structural information of the pectins in peach flesh.

Further structural details showed a periodic height fluctuation along the contour of the chains. This was observed in almost all chains from 3D height images. A typical example is shown in Fig. 1f. The figure shows that 3D height AFM images of pectin chains from peaches appeared as helical structures, similar to xanthan that was reported by Morris et al. (1999, 2001). The surfaces of WSP in soft cultivar peaches looked knobbly (Fig. 1c and d), similar to myosin filaments reported by Iwasaki et al. (2005).

Fig. 4 shows cross-section analysis of pectin chains and strands. For any AFM image (Fig. 4c, for instance), a cross-sectional line can be drawn across the image at any place and direction, and the height profile of the cross-section highlighted in the image (Fig. 4a) is shown above the AFM image (Fig. 4c). The software allowed a fixed, movable line to be drawn across a section. The results of the portion of the cross-section between the two selected cursors are shown in part of Fig. 4b. The power spectrum along the cross-section is displayed in part of Fig. 4d. Up to three pairs of cursors can be applied on the line section and the results are displayed as red, blue and black part in the part of Fig. 4e (Yang et al., 2006c).

AFM imaging offers the opportunity to characterize the chelator (ch), sodium carbonate (so), and integral heterogeneous structures of pectins, including linear chains, branch points, aggregates (ag) and chain lengths. Moreover, cleavage points (cp), branch structures (br), long chains (lc), short chains (sc), multiply branched chains (mb) as well as the releasing point (rp) of pectin chains released from the CDTA chelator were identified and shown in both the CSP and SSP images (Yang et al., 2006c). It should be noted that cp means a cleavage point between pectin molecules while rp denotes a releasing point of pectin from the chelator. The figures show that some chains crossed over one another to form greater heights. These cross-over regions were characterized by brighter dots in the height images (Roesch et al., 2004). The shapes and dimensions of the same kind of pectins were highly polydisperse,

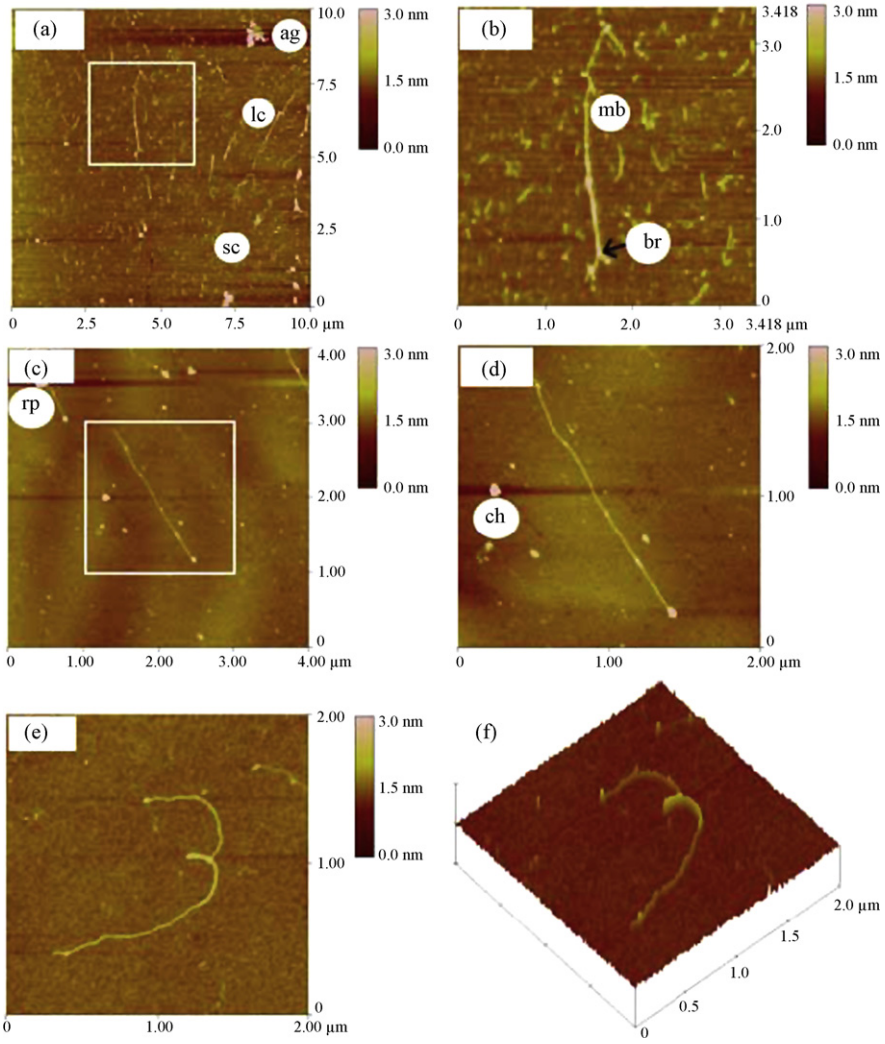

Fig. 2. AFM images of chelate soluble pectin (CSP) from soft and crisp peach cultivars. (a) CSP from crisp peaches; (b) an enlarged image of (a); (c) a typical CSP from soft peaches; (d) an enlarged image of (c); (e) an untypical image of CSP from soft peaches; (f) corresponding 3D image of Fig. 1e. *Note*: ag: aggregates; br: branch structures; ch: chelator, CDTA; lc: long chains; mb: multiple branched chains; rp: releasing point; sc: short chains.

suggesting these pectins might not be just individual molecules but aggregates. The WSP chains of crisp peaches (Fig. 1a and b) appeared to be straighter than those of soft ones (Fig. 1c–f), indicating that the general structure of the former was stiffer (Ikeda et al., 2004a). Furthermore, a typical image of the SSP of crisp peaches (Fig. 3a) shows a mixed population of single chains and aggregates (Fig. 3a) that were identified from height measurement with section analysis. The aggregates existed even at low concentrations where few single chains were seen from the images, indicating that they were not just the result of aggregation of polymers from evaporation of water during drying on the mica before imaging, but to a large extent the result of the strong intermolecular interaction that held these aggregates together (Round et al., 1997, 2001).

3.2. Quantitative results

Generally speaking, the difference in the lengths of the same kinds of pectins between the two cultivars was larger than that of the widths and heights. For example, most of the widths of the pectins in both cultivars were about 20–100 nm, and almost all the heights of the pectins (WSP, CSP and SSP) in the two cultivars were about 1–5 nm, most of the pectin heights were about 2.5–3 nm (Fig. 4), and only a small part of the chains were <1 nm. In general, the height within a chain was fairly constant and uniform, as was that of the chains of xylogulcan, gellan and proteins that have been reported previously (Ikeda and Morris, 2002; Ikeda et al., 2004b). The result indicates that there was no statistical difference among these chain heights, and it also indicates that the chains might be native monomers or they did not aggregate in the *Z* scale. At higher magnification, variations in the height of individual chains were clearly seen (Figs. 1f, 2f and 3c) (Ikeda and Shishido, 2005).

The lengths of WSP, CSP and SSP between the two peach cultivars had different tendencies. For WSP and CSP, there was not much difference between the two cultivars. The average length of WSP in firm peaches was about 1.3 μm (0.3–4.0 μm), and it was 2.5 μm (0.8–4.2 μm) in soft peaches. For CSP, many short rods and some longer chains were seen in the images (Fig. 2a and b, for instance). The lengths of individual chains in both cultivars varied greatly, approximately from 0.1–3.0 μm, suggesting a wide range of molecular weight distribution. Compared with WSP and CSP, the distribution of SSP lengths of the observable single chains showed a large difference between the two cultivars (Fig. 3a and b for crisp peaches, and Fig. 3d and e for soft peaches). The SSP chain lengths of the crisp peaches were significantly longer than those in the soft cultivar. The lengths of SSP chains of crisp peaches were 249 ± 256 nm ($n = 138$), while they were only 57 ± 27 nm ($n = 40$) in

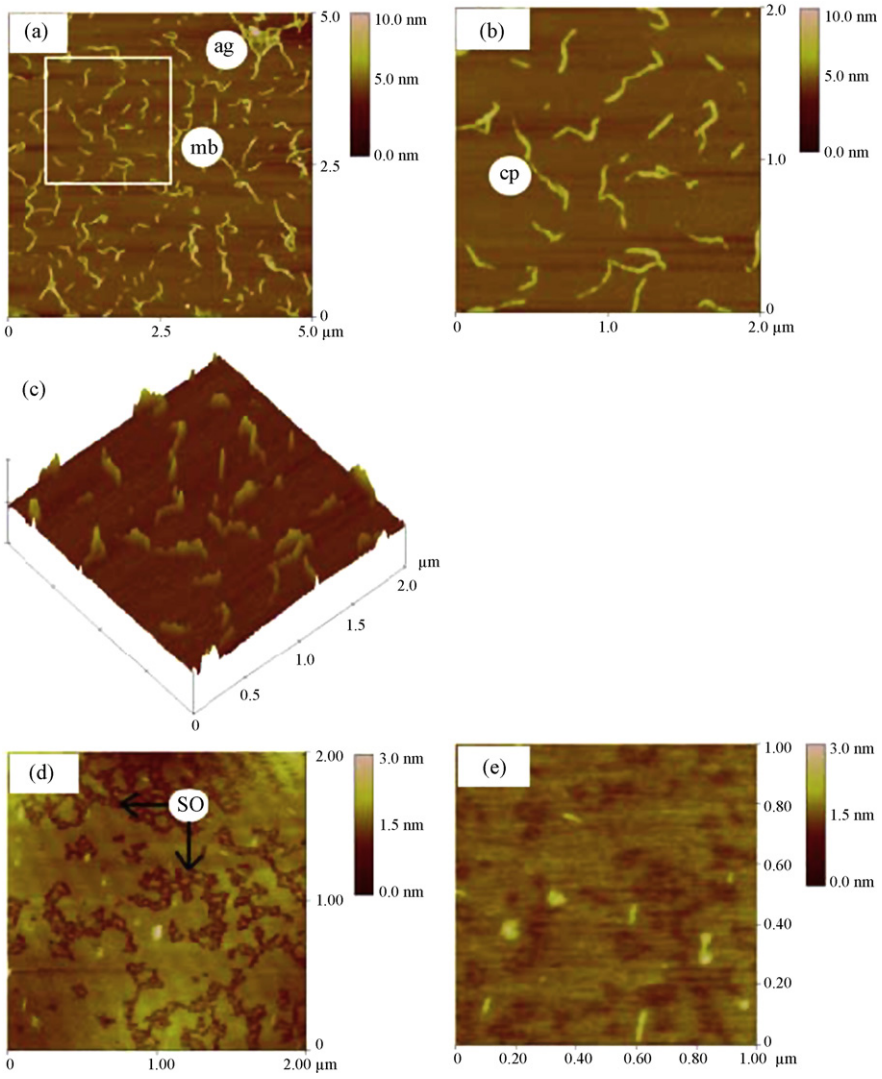

Fig. 3. AFM images of sodium-carbonate soluble pectin (SSP) from soft and crisp peach cultivars. (a) SSP from crisp peaches; (b) an enlarged image of (a); (c) corresponding 3D image of (b); (d) SSP from the soft peaches; (e) another image of SSP from the soft peaches. *Note*: ag: aggregates; cp: cleavage point; so: sodium carbonate; mb: multiple branched chains.

the soft peaches. The distributions of the SSP lengths for the two cultivars are shown in Figs. 5 and 6.

4. Discussion

AFM imaging can be performed in air or in liquid. For imaging in liquid, butanol is one of the most widely used liquids for improving AFM resolution since it is a poor solvent for polysaccharides, thus it retains the samples on the mica surface during scanning and effectively decreases the capillary-induced adhesive forces between the sample and the tip (Morris et al., 1999). Therefore, AFM imaging in butanol or other alcohols could decrease the lateral force during scanning. However, butanol or other alcohols were not used in our study since they precipitated polysaccharides and might affect the pectin structures (Decho, 1999). Therefore, AFM imaging pectin was conducted in air.

Pectin, as a polysaccharide, is chemically composed of monosaccharides. The measured vertical heights for the pectin chains corresponded to different aggregation status. Pectin is a highly heterogeneous polysaccharide and therefore it is natural that there was a big variation (1–5 nm) of chain heights. Single stranded chains have heights of about 0.5 nm, and association of single chains into double strands was about 1 nm. Pectins with different values of heights corresponded to different associations of single monosaccharide chains (McIntire and Brant, 1999).

From the results, pectin molecules showed strong binding ability to the mica surfaces and could not be washed away by water within a certain speed, indicating strong adsorption of mica to the pectin molecules. The actions between the pectin and mica might be electronic attraction as with other macromolecules. This is important in our experiment, because we imaged the pectin molecules without dialyzing out the salt, suggesting that molecular manipulation should be applied to obtain the images with pectin. In this situation, charged pectin showed strong binding ability to mica surfaces and could not be washed away by water or wiped out by molecular combing during molecular manipulation. If electrically neutral polymers were imaged, we could not apply the two molecular manipulation techniques since the macromolecule would be washed away or wiped out due to the weak binding ability with mica. For electrically neutral polymers, we have to dialyze out the salt and then deposit the solution on the mica surface and dry it in air, then image the sample by AFM. If the pectin and mica have the same charge, pectin solution can be dropped on the mica surface and air-dried, the dried sample can absorb well and thus be

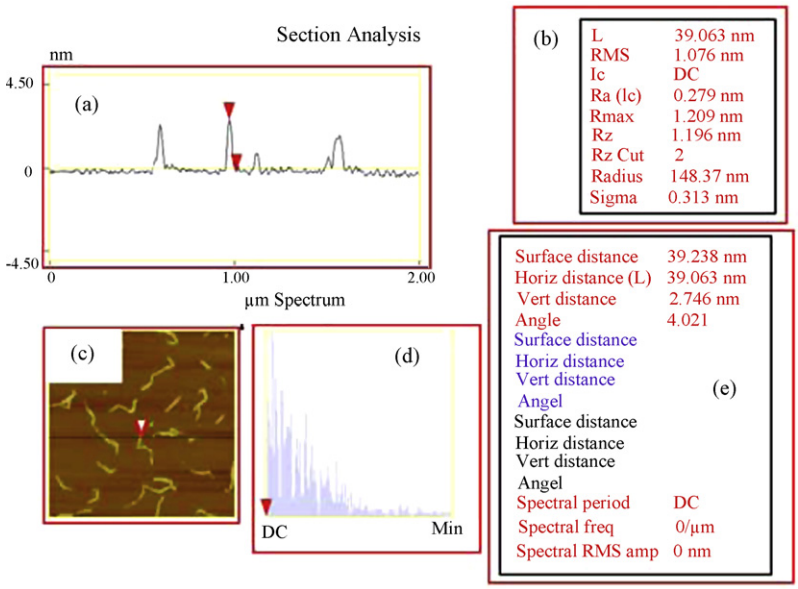

Fig. 4. Cross-section analysis of pectin chains: (a) the height profile along a cross-sectional line; (b) the dimension measurements of the portion of the cross-section between the two colored cursors; (c) an sample of AFM image; (d) the power spectrum along the cross-section; (e) dimension measurements of up to three pairs of cursors that placed on the line section. (For interpretation of the references to color in the text, the reader is referred to the web version of the article.)

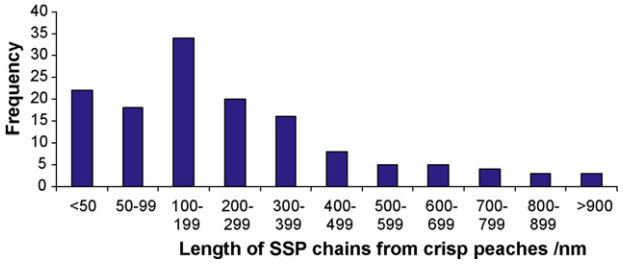

Fig. 5. Frequencies of sodium-carbonate soluble pectin (SSP) chain lengths from the crisp peaches.

imaged. But in this situation, the two molecular manipulation techniques cannot be applied and we should separate the pectin with salt before preparation of the samples to obtain full images of pectin chains. When dried from water, for highly flexible polysaccharides, such as pectins, the molecules showed random coil structures if imaged without any manipulation. Pectin chains tended to form discrete circular structures and the AFM images were globular structures representing time averaged pictures of the molecular nanostructures (Yang et al., 2006a). Fishman et al. (2004) observed that the branched structures of peach pectins were comprised of rods, segmented rods, and kinked rods that were held together by noncovalent interactions. These interactions might partly be

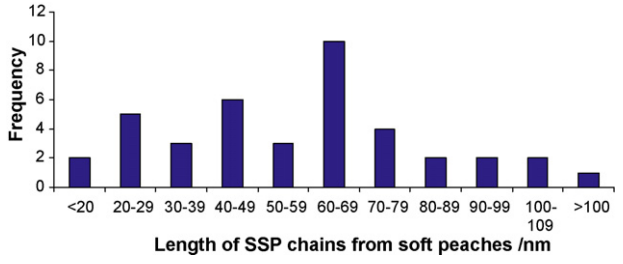

Fig. 6. Frequencies of sodium-carbonate soluble pectin (SSP) chain lengths from the soft peaches.

from the air-drying operation after deposition on mica because of an increased polysaccharide concentration (Fishman et al., 1993a; Ikeda and Shishido, 2005). Some of the aggregates after drying were composed of short rod-like or segmented rod-like subunits. Our results are consistent with the concept that peach cell wall pectin comprises a hierarchy of aggregates held together by noncovalent forces. These rods and segmented rods were joined together to form integrated networks and these networks can be opened by modified molecular combing or fluid fixation techniques that we developed (Fishman et al., 1992; Yang et al., 2006a). When these techniques were applied, the pectin chains were straightened and characteristic dimensions could be calculated. Generally speaking, pectin molecules could be stretched to some degree, but the extent of stretching depended on cultivars and kinds, and it was hard to get wholly stretched molecules without affecting the genuine nanostructures, as was seen in Figs. 1–3 (Yang et al., 2006a). The chain straightness is one of the fundamental properties of macromolecular chains and can provide useful information about the molecules (Morris et al., 2001). Even though the molecular combing technique was not fully homogeneous across the slide, the images of the pectin chains were similar and the quantitative information was stable for the same sample. And the general tendency of the pectin morphology imaged was consistent by this technology. Most importantly, it did not alter the quantitative information of the heights of the pectin chains. Therefore, this technology has been widely applied in AFM imaging of biological samples since it was invented (Yang et al., 2006a).

Whether the pectin chains were in helices can be discriminated by the height information of the chains. If the heights of the chains were larger than 0.5 nm, the chains might have a helix structure, if not, the chains would be non-helix forming molecules (McIntire and Brant, 1999). Other additional information includes the chain height periodicity, the height variations, and the occasionally branching structures. The combination of the chain heights, the chain height periodicity, the height variations, and the occasionally branching structures indicates that the pectin chains of the two cultivars were helical structures (Arnaudov et al., 2003). The AFM images showed that a small number of the CSP and SSP chains of the crisp peaches had branched structures, consistent

with a previous report in tomato (Round et al., 1997), while few or no branched structures existed in the soft peaches. Gunning et al. (2003) reported two different types of branching patterns for amylose: a linear backbone containing a single long branch and a linear backbone containing multiple short branches; the CSP and SSP of crisp peaches here had similar structures.

It should be noted that there were several factors that could affect the accuracy of the measured dimensions of pectins. First, the width of pectins in the AFM images can be influenced by probe-broadening effect and the level of influence depended on many factors including shape, size and property of the tip, and the surface characteristics of the sample (Ikeda and Shishido, 2005). If the sample being measured sits on the surface, the side of the probe might cause the tip to rise before it reaches the front edge of the sample and to fall after it passes over the back edge of the sample. Then, the measured dimensions would be larger than the genuine dimensions. This effect was called "probe broadening". Other possible sources of artifacts were from sample dehydration during imaging, and from contamination between the tip and the sample, which could be creased by timely changing of tips (Fishman et al., 2004). Generally, in the *Z* scale, the main source of artifacts was the tip-sample interaction. The sample might be compressed due to an interaction between the sample and the AFM tip. Such an effect could lead to up to a 60% underestimation of the actual height of the observed chains as reported by previous research. The chain being compressed can provide much valuable information about the chain properties. AFM can record the distance (height mode images) as well as the force (force spectroscopy) between the tip and sample. In our current research, only height mode images (providing the dimension information of the sample) were analyzed. If we want to analyze the physiochemical properties of macromolecules, we can analyze the results of force spectroscopy, which serves as a bridge connecting nanostructure with physiochemical properties of macromolecules (Watabe et al., 2006; Yang et al., 2007). In fact, the experimentally observed height increase at an overlap was often less than two fold (but always greater than 1.5×) due to compression of the polymers by the AFM tip during scanning. Measuring the heights of apparent branching points ensured that superimposed polymers could be rejected from the analysis and only true branch points were included (Round et al., 2001). For pectin widths, the main source of artifacts was probe broadening. According to the report by McMaster et al. (1999), width observed from AFM for a cylindrical object is typically three times greater than the actual value. In our results, the observed widths were almost an order of magnitude larger than the measured heights. This was due to probe broadening effects (Fishman et al., 2004), and it also indicates that the effect of probe broadening was much larger than that of the interaction between tip and the sample.

The textural differences between different cultivars were not the same as those between different ripening stages in the same cultivar. For the latter, many enzymes and biochemical processes may take place, while for the textural differences between different cultivars for the similar ripeness stages, for instance, both at full ripeness in our experiment, the cell wall skeleton itself may contribute a lot. Therefore, the results of different CSP between different ripening stages in the same cultivar might not be comparable with our current research (Hegde and Maness, 1998; Brummell et al., 2004). Fishman et al. (1993b) investigated the pectin difference between non-melting flesh (crisp) peach and melting flesh (soft) peach, and showed changes in molecular weight of CSP and alkaline-soluble pectin (ASP, similar to SSP in our experiment) during storage. On day 6 during storage, the ASP between the two cultivars showed a large difference, while the CSP between the two cultivars had similar molecular weights, which was consistent with our results (the peaches in our experiments were also at day 6 during storage).

We can draw the conclusion that the differences from AFM images are actual differences in the in vivo polymers rather than from the differences in the cell walls that subsequently modify the nature and efficiency of the extraction procedures. The main reason was that the two peach cultivars were both at the full ripeness stage. In the report from Hegde and Maness (1998), the peaches chosen for cell wall preparation represented different commercial maturity stages of threshold mature, firm ripe, and soft ripe. Therefore, the difference between the peaches in their report might be from the subsequent modification of the nature and efficiency of the extraction procedure. However, for the two peach cultivars at the full ripeness stage in our experiment, there was not much difference between the nature and efficiency of extraction from cell walls.

There were two kinds of common evidence that could certify that the linear structure from AFM images was pectin molecules and not fragments from the cell wall. One is by measuring the intrinsic viscosity of the sample, and our previous experiments tested two similar cultivars of peaches. The results were comparable with tomato paste pectin, citrus pectin (Chou and Kokini, 1987), and orange peel pectin (Kar and Arslan, 1999), which verified that the extracted samples using this method were pectin molecules rather than fragments from the cell wall. Other evidence comes from the AFM images themselves. For AFM images of fragments from the cell wall, there exists a laminated structure with fibers in different layers showing different directions. And the AFM images can show polylaminate structures of cell walls, which are totally different from our current images (Kirby et al., 1996).

Even though the molecular weight can be calculated roughly from AFM images, it is only effective to a certain degree. The reason is that pectin is a highly heterogeneous polysaccharide, and the visible parts from AFM images are only parts of the molecules. Some small molecules can be imaged but are not visible or statistically analyzed because of the limitation of eyes or software. Pectin itself contains short neutral sugar side chains as well as long branches, and the presence of this small fraction of branched molecules will alter the viscosity-molecular weight relationships (Morris et al., 2001).

The CDTA extraction released CSP from the cell wall by chelating calcium. The freed CSP was cross-linked by calcium and was released mainly from the middle lamella of the flesh. The following extraction with Na_2CO_3 was considered to free SSP by breaking ester linkages and release neutral sugar-rich pectins from the primary cell wall (Round et al., 2001). The large difference in SSP chain lengths between the two cultivars indicates that neutral sugar-rich pectins from the primary cell wall of peach flesh was the main difference in pectins between the soft and the crisp peach cultivars.

5. Conclusion

Two peach cultivars (soft and crisp) were selected to analyze the nanostructures of pectins in order to illustrate the fundamental reason for differences in firmness. WSP, CSP and SSP were extracted and the nanostructures were performed and analyzed using AFM. The results revealed that a large difference existed in the lengths of SSP chains between the two cultivars. The average lengths of SSP in the crisp and soft cultivars were 249 nm and 57 nm, respectively. There were no large differences for lengths of WSP and CSP, and no statistical differences for chain heights and widths of the three kinds of pectins between the two cultivars. The results demonstrate that neutral sugar-rich pectins from the primary cell wall of peach flesh might be the source of the main differences in pectins and firmness between the two peach cultivars.

Acknowledgements

Project 30600420 supported by National Natural Science Foundation of China contributed to this research. The authors thank Hui Liu and Jinjing Zuo for assistance in extracting the pectin samples.

References

Ali, Z.M., Chin, L.H., Lazan, H., 2004. A comparative study on wall degrading enzymes, pectin modifications and softening during ripening of selected tropical fruits. Plant Sci. 167, 317–327.

Arnaudov, L.N., de Vries, R., Ippel, H., van Mierlo, C.P., 2003. Multiple steps during the formation of β-lactoglobulin fibrils. Biomacromolecules 4, 1614–1622.

Brummell, D.A., Cin, V.D., Cristo, C.H., Labavitch, J.M., 2004. Cell wall metabolism during maturation, ripening and senescence of peach fruit. J. Exp. Bot. 55, 2029–2039.

Chou, T.D., Kokini, I.L., 1987. Rheological properties and conformation of tomato paste pectins, citrus and apple pectins. J. Food Sci. 52, 1658–1664.

Decho, A.W., 1999. Imaging an alginate polymer gel matrix using atomic force microscopy. Carbohydr. Res. 315, 330–333.

Deng, Y., Wu, Y., Li, Y., 2005. Changes in firmness, cell wall composition and cell wall hydrolases of grapes stored in high oxygen atmospheres. Food Res. Int. 38, 769–776.

Fishman, M.L., Cooke, P.H., Coffin, D.R., 2004. Nanostructure of native pectin sugar acid gels visualized by atomic force microscopy. Biomacromolecules 5, 334–341.

Fishman, M.L., Cooke, P., Levaj, B., Gillespie, D.T., Sondey, S.M., Scorza, R., 1992. Pectin microgels and their subunit structure. Arch. Biochem. Biophys. 294, 253–260.

Fishman, M.L., Cooke, P., Hotchkiss, A., Damert, W., 1993a. Progressive dissociation of pectin. Carbohydr. Res. 248, 303–316.

Fishman, M.L., Levaj, B., Gillespie, D., 1993b. Changes in the physico-chemical properties of peach fruit during on-tree ripening and storage. J. Am. Soc. Hort. Sci. 118, 343–349.

Gunning, A.P., Giardina, T.P., Faulds, C.B., Juge, N., Ring, S.G., Williamson, G., Morris, V.J., 2003. Surfactant-mediated solubilisation of amylose and visualisation by atomic force microscopy. Carbohydr. Polym. 51, 177–182.

He, S., Feng, G., Yang, H., Wu, Y., Li, Y.F., 2004. Effects of pressure reduction rate on quality and ultrastructure of iceberg lettuce after vacuum cooling and storage. Postharvest Biol. Technol. 33, 263–273.

Hegde, S., Maness, N.O., 1998. Changes in apparent molecular mass of pectin and hemicellulose extracts during peach softening. J. Am. Soc. Hort. Sci. 123, 445–456.

Ikeda, S., Nitta, Y., Kim, B.S., Temsiripong, T., Pongsawatmanit, R., Nishinari, K., 2004b. Single-phase mixed gels of xyloglucan and gellan. Food Hydrocolloid. 18, 669–675.

Ikeda, S., Shishido, Y., 2005. Atomic force microscopy studies on heat-induced gelation of curdlan. J. Agric. Food Chem. 53, 786–791.

Ikeda, S., Morris, V.J., 2002. Fine-stranded and particulated aggregates of heat-denatured whey proteins visualized by atomic force microscopy. Biomacromolecules 3, 382–389.

Ikeda, S., Morris, V.J., Nishinari, K., 2001. Microstructure of aggregated and nonaggregated κ-carrageenan helices visualized by atomic force microscopy. Biomacromolecules 2, 1331–1337.

Ikeda, S., Nitta, Y., Temsiripong, T., Pongsawatmanit, R., Nishinari, K., 2004a. Atomic force microscopy studies on cation-induced network formation of gellan. Food Hydrocolloid. 18, 727–735.

Iwasaki, T., Washio, M., Yamamoto, K., 2005. Atomic force microscopy of thermally treated myosin filaments. J. Agric. Food Chem. 53, 4592–4598.

Kar, F., Arslan, N., 1999. Effect of temperature and concentration on viscosity of orange peel pectin solutions and intrinsic viscosity-molecular weight relationship. Carbohyd. Polym. 40, 277–284.

Ketsa, S., Chidtragool, S., Klein, J.D., Lurie, S., 1999. Firmness, pectin components and cell wall hydrolases of mango fruit following low-temperature stress. J. Hortic. Sci. Biotechnol. 74, 685–689.

Kirby, A.R., Gunning, A.P., Waldron, K.W., Morris, V.J., Ng, A., 1996. Visualization of plant cell walls by atomic force microscopy. Biophys. J. 70, 1138–1143.

McIntire, T.M., Brant, D.A., 1999. Imaging of carrageenan macrocycles and amylose using noncontact atomic force microscopy. Int. J. Biol. Macromol. 26, 303–310.

McMaster, T.J., Miles, M.J., Kasarda, D.D., Shewry, P.R., Tatham, A.S., 1999. Atomic force microscopy of A-gliadin fibrils and in situ degradation. J. Cereal Sci. 31, 281–286.

Morris, V.J., Mackie, A.R., Wilde, P.J., Kirby, A.R., Mills, E.C., Gunning, A.P., 2001. Atomic force microscopy as a tool for interpreting the rheology of food biopolymers at the molecular level. Lebensm. Wiss. Technol. 34, 3–10.

Morris, V.J., Kirby, A.R., Gunning, A.P., 1999. Atomic Force Microscopy for Biologists. Imperial College Press, London.

Reed, J., Singer, E., Kresbach, G., Schwartz, D.C., 1998. A quantitative study of optical mapping surfaces by atomic force microscopy and restriction endonuclease digestion assays. Anal. Biochem. 259, 80–88.

Roesch, R., Cox, S., Compton, S., Happek, U., Corredig, M., 2004. κ-Carrageenan and β-lactoglobulin interactions visualized by atomic force microscopy. Food Hydrocolloid. 18, 429–439.

Round, A.N., MacDougall, A.J., Ring, S.G., Morris, V.J., 1997. Unexpected branching in pectin observed by atomic force microscopy. Carbohydr. Res. 303, 251–253.

Round, A.N., Rigby, N.M., MacDougall, A.J., Ring, S.G., Morris, V.J., 2001. Investigating the nature of branching in pectin by atomic force microscopy and carbohydrate analysis. Carbohydr. Res. 331, 337–342.

Watabe, H., Nakajima, K., Sakai, Y., Nishi, T., 2006. Dynamic force microscopy on a single polymer chain. Macromolecules 39, 5921–5925.

Yang, H., Wang, Y., Lai, S., An, H., Li, Y., Chen, F., 2007. Application of atomic force microscopy as a nanotechnology tool in food science. J. Food Sci. 72, R65–R75.

Yang, H., Lai, S., An, H., Li, Y., 2006c. Atomic force microscopy study of the ultrastructural changes of chelate-soluble pectin in peaches under controlled atmosphere storage. Postharvest Biol. Technol. 39, 75–83.

Yang, H., An, H., Li, Y., 2006a. Manipulate and stretch single pectin molecules with modified molecular combing and fluid fixation techniques. Eur. Food Res. Technol. 223, 78–82.

Yang, H., An, H., Feng, G., Li, Y., 2005b. Visualization and quantitative roughness analysis of peach skin by atomic force microscopy under storage. LWT-Food Sci. Technol. 38, 571–577.

Yang, H., An, H., Feng, G., Li, Y., 2005a. Atomic force microscopy of the water-soluble pectin of peaches during storage. Eur. Food Res. Technol. 220, 587–591.

Yang, H., Feng, G., An, H., Li, Y., 2006b. Microstructure changes of sodium carbonate-soluble pectin of peach by AFM during controlled atmosphere storage. Food Chem. 94, 179–192.

Yang, S., Wang, P., Shan, L., Cai, C., Zhang, B., Zhang, W., Li, X., Ferguson, I., Chen, K., 2008. Expression of expansin genes during postharvest lignification and softening of 'Luoyangqing' and 'Baisha' loquat fruit under different storage conditions. Postharvest Biol. Technol. 49, 46–53.

Zhang, L., Chen, F., An, H., Yang, H., Sun, X., Guo, X., Li, L., 2008. Physicochemical properties, firmness, and nanostructures of sodium carbonate-soluble pectin of 2 Chinese cherry cultivars at 2 ripening stages. J. Food Sci. 73, N17–N22.

Zhou, H., Sonego, L., Khalchitaski, A., Ben-Arie, R., Lers, A., Lurie, S., 2000. Cell wall enzymes and cell wall changes in 'Flavortop' nectarines: mRNA abundance, enzyme activity, and changes in pectic and neutral polymers during ripening and in wolly fruit. J. Am. Soc. Hortic. Sci. 125, 630–677.

Zhou, R., Li, Y., 2007. Texture analysis of MR image for predicting the firmness of Huanghua pears (*Pyrus pyrifolia* Nakai, cv. Huanghua) during storage using an artificial neural network. Magn. Reson. Imaging 25, 727–732.